Solid State Nuclear Magnetic Resonance 34 (2008) 180–185

Contents lists available at ScienceDirect

Solid State Nuclear Magnetic Resonance

journal homepage: www.elsevier.com/locate/ssnmr

Study of molecular dynamics and cross relaxation in tetramethylammonium hexafluorophosphate $(CH_3)_4NPF_6$ by ^1H and ^{19}F NMR ☆

K.J. Mallikarjunaiah [a,1], R. Damle [a,*], K.P. Ramesh [b]

[a] Department of Physics, Bangalore University, Bangalore 560 056, India
[b] Department of Physics, Indian Institute of Science, Bangalore 560 012, India

ARTICLE INFO

Article history:
Received 3 March 2008
Received in revised form
30 May 2008
Available online 28 August 2008

Keywords:
^1H ^{19}F NMR
Internal motions
Spin lattice relaxation time
Second moment

ABSTRACT

$(CH_3)_4NPF_6$ is studied by NMR measurements to understand the internal motions and cross relaxation mechanism between the heterogeneous nuclei. The spin lattice relaxation times (T_1) are measured for ^1H and ^{19}F nuclei, at three (11.4, 16.1 and 21.34 MHz) Larmor frequencies in the temperature range 350–50 K and ^1H NMR second moment measurements at 7 MHz in the temperature range 300–100 K employing home made pulsed and wide-line NMR spectrometers. ^1H NMR results are attributed to the simultaneous reorientations of both methyl and tetramethylammonium groups and motional parameters are evaluated. ^{19}F NMR results are attributed to cross relaxation between proton and fluorine and motional parameters for the PF_6 group reorientation are evaluated.

1. Introduction

APF_6 (A = K, Na, Rb, Cs, $C_5H_{10}NH_2$, $C_4H_8NH_2$, $C(NH_2)_3$, NH_4 and $N(CH_3)_4$) compounds are interesting due to the various phase transitions they exhibit and also due to the complex reorientational dynamics of the molecular groups [1–7]. NMR studies on alkali hexafluorophosphates (HFP) have shown that the reorienting groups are sensitive to the physical state of the sample [8]. PF_6 reorientations have been commonly observed and the temperature of their occurrence is dependent on the alkali ion radius and also on the defects. The objective of the present work is to examine the effect of changing the alkali by symmetric cation like TMA and to look for the changes in the reorientational dynamics.

In the present study, the proton and fluorine spin lattice relaxation time (T_1) and proton second moment measurements are undertaken in tetramethylammonium hexafluorophosphate (hereafter abbreviated as TMA-HFP) to understand (1) the dynamics of reorienting groups CH_3, $N(CH_3)_4$ and PF_6, (2) to explore the proton–fluorine dipolar interactions if present, (3) to look into the effect of hydrogen bond in hindering the motional behaviour of the BF_6 (where B = P, Sb and As) groups [9] and (4) to look for the coexistence of the two phases. Further ^{31}P T_1 studies [10] in TMA-HFP had shown the existence of two phases with and without imperfections. Our aim is to study these phases and their effect using ^{19}F and ^1H NMR studies. TMA-HFP is a promising candidate for technological applications viz., in high energy density battery applications, as electrolyte for the preparation of the films, to make semiconductor films, as corrosive resistant material and in making opaque inkjet ink compositions [11]. The present studies may help in crystal engineering and material preparation.

2. Earlier studies

Wang et al. [12] have reported the room temperature crystal structure of TMA-HFP to be tetragonal (P4/nmm). Even though the N-atom formally has a distorted tetrahedral symmetry $\bar{4}2m - D_{2d}$, the cation can nevertheless considered to be tetrahedral within experimental accuracy and the P-atom has square–pyramidal symmetry, 4 mm. Infrared and Raman studies [7] have not revealed any phase transitions with temperature. Reynhardt et al. [10] have carried out ^{31}P NMR, differential scanning calorimetry (DSC) and X-ray powder diffraction measurements as a function of temperature. DSC measurements from 120 to 800 K have revealed three endothermic transitions at 770, 789 and 795 K. However, DSC thermograms do not show any low temperature (<220 K) phase changes. X-ray diffraction experiments revealed two phases, namely room temperature phase (P) and low temperature phase (I). Room temperature phase (P) exhibits a tetragonal unit cell with $a = 8.559$ Å and $c = 6.136$ Å, while the low temperature (below 220 K) phase appears to have a hexagonal unit cell with

☆ NMR study of molecular dynamics in TMA-HFP.

* Corresponding author. Fax: +91 080 2321 1012.
E-mail address: ramkrishnadamle@bub.ernet.in (R. Damle).
[1] Present address: Department of Chemistry, University of Arizona, Tucson, AZ-85721.

0926-2040/$ - see front matter © 2008 Elsevier Inc. All rights reserved.
doi:10.1016/j.ssnmr.2008.08.002

$a = 13.507$ Å and $c = 7.328$ Å. Both the phases coexist in the temperature range 160–220 K and above 220 K, only P phase stabilizes. On lowering the temperature below 210 K, the X-ray diffractogram has shown additional six peaks indicating the appearance of a new phase coexisting with room temperature phase. The additional peaks appearing below 210 K represent a new diffraction plane which is indexed by hexagonal unit cell. Further, the new peak intensities increase with decreasing temperature and remain constant below 150 K. ^{31}P NMR T_1 studies as a function of temperature at 81 MHz, revealed a single minimum of about 100 ms around 150 K, which is explained in terms of Miller and Gutowsky's two-phase model [1]. They concluded that TMA-HFP contains two phases one with imperfections and another without imperfections. ^{31}P NMR T_1 analysis yield an activation energy of 15 ± 2 kJ/mol, $\tau_{co} = (6 \pm 2) \times 10^{-15}$ s for isotropic reorientation of all PF_6 ions.

3. Experimental

In the present study, commercially available TMA-HFP from Aldrich Chemicals [558-32-7] is used directly without further purification. The compound is finely powdered and vacuum-sealed into glass ampoules of 5 mm diameter in helium atmosphere and then used for NMR measurements. ^{1}H NMR second moment (M_2) measurements are carried out, as a function of temperature in the range 300–77 K at 7 MHz, using a home made wide-line NMR spectrometer described elsewhere [13]. Temperature of the sample is controlled and measured using a home made gas flow cryostat along with a Pt 100 sensor. Second moment is calculated from the derivative of the absorption signal recorded using lock-in detection.

Both ^{1}H and ^{19}F NMR spin lattice relaxation time (T_1) measurements are carried out, as a function of temperature, at three Larmor frequencies 21.34 MHz, 16.1 MHz and 11.4 MHz for proton and 21.34 MHz and 16.1 MHz for fluorine. T_1 measurements are made as a function of temperature in the range 350–50 K using a home made pulsed NMR spectrometer described elsewhere [14]. Inversion recovery pulse sequence is used for the measurement of T_1 (when $T_1 < 1$ s) and at higher temperatures (when $T_1 > 1$ s) saturation burst sequence is used. For both the nuclei studied (^{1}H and ^{19}F), the magnetisation recovery is found to be single exponential within the experimental error throughout the temperature range studied.

4. Results and discussion

4.1. Second moment studies

Variation of second moment as a function of temperature in the range 300–77 K is shown in Fig. 1. M_2 remains almost constant (3 ± 0.2 G^2) in the temperature range 300–180 K. Below 180 K, the signal starts broadening and second moment increases monotonically with a decrease in intensity. The signal could be detected down to only 155 K with a second moment of 18 ± 1 G^2. Below this temperature, due to poor signal to noise ratio, the second moment measurement was impossible. Attempt to measure second moment by directly immersing the sample in liquid nitrogen (77 K) also failed due to poor signal to noise ratio.

The theoretical second moment for a rigid molecular group in the crystal lattice can be calculated using the methods of moments given by Van Vleck [15]. There are many second moment simulation studies reported in the literature including those for tetramethylammonium ion in different complexes [16–23]. Following this, the second moment can be calculated

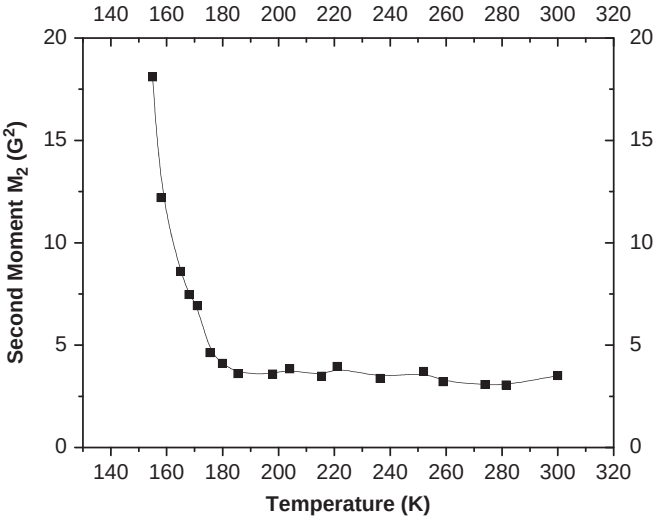

Fig. 1. ^{1}H NMR second moment data for TMA-HFP at 7 MHz in the temperature region 300–155 K; the line is a guide to the eye.

for a rigid $(CH_3)_4N$ ion using the formula

$$M_2 = \frac{9}{10}\frac{\gamma^2\hbar^2}{r^6} + \frac{81}{20}\frac{\gamma^2\hbar^2}{R^6} + M_{HT}, \quad (1)$$

where $\gamma = 2.675 \times 10^4$ G^{-1} s^{-1} is the nuclear gyromagnetic ratio of protons and M_2 is expressed in G^2. Following Albert et al. [24], for second moment calculations we have used $r = 1.78$ Å as the distance between the protons belonging to the same CH_3 group and $R = 3.04$ Å as the average distance between the protons belonging to different CH_3 groups (but within the same TMA group). The calculated intra-CH_3 contribution is about 22.4 G^2 and inter-CH_3 contribution of the same ion is about 3.88 G^2. Considering the high temperature residual second moment M_{HT} (due to inter-CH_3 of the other ion) to be 1 G^2 [25], the calculated total second moment is about 28 G^2 [21]. In the present investigation, the observed M_2 is only 18 G^2 at 155 K, the lowest temperature of measurement. This would imply that, only certain reorienting groups are frozen while the others are still reorienting even at 155 K and hence the corresponding activation energy for these reorientations has been estimated as 24 kJ/mol using the formula $E_a = 155\,T_c$ kJ/mol, where T_c is taken as 155 K. The observed plateau second moment of about 3 G^2 in the high temperature region suggests that both TMA and methyl groups reorientations are active down to 180 K, below which, both the groups start freezing. Generally, two plateau regions are expected for TMA compounds. This investigation shows a single plateau in second moment indicating that the correlation frequencies for the two motions are quite close to each other [22]. Similar behaviour has been observed in $(CH_3)_4NCdCl_3$ [21], $(CH_3)_4NCl$ [22], $((CH_3)_4N)_2MX_6$ (M = Pt, Te and Sn, X = Cl and Br) [26,27], $((CH_3)_4N)_2SeO_4$ [28] and $(CH_3)_4NGeCl_3$ [29].

4.2. Spin lattice relaxation time studies

Fig. 2 shows the variation of ^{1}H and ^{19}F NMR spin lattice relaxation times (T_1) with inverse temperature ($1000/T$) over the entire temperature range studied. The T_1 data are analysed in two parts: (a) ^{1}H NMR spin lattice relaxation time as shown separately in Fig. 3 and (b) ^{19}F, NMR spin lattice relaxation time as shown separately in Fig. 4.

(a) ^{1}H *NMR T_1 analysis*: Fig. 3 shows the ^{1}H NMR spin lattice relaxation time data at three Larmor frequencies (11.4, 16.1 and 21.34 MHz). Initially T_1 decreases with decrease in temperature

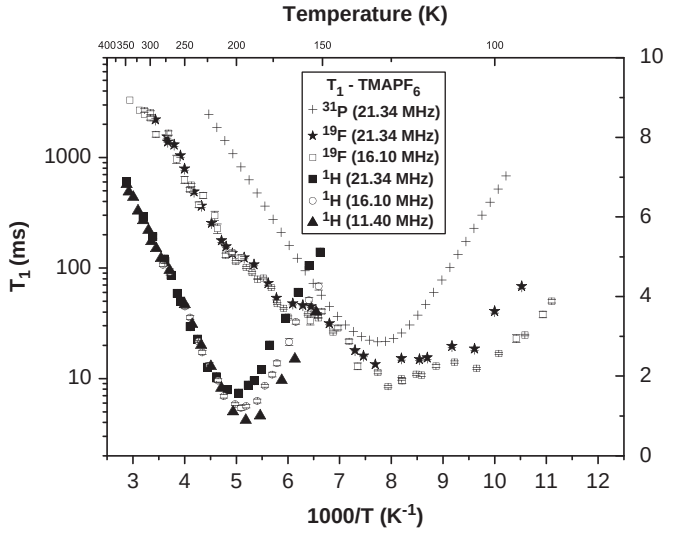

Fig. 2. ^{1}H (11.4, 16.1 and 21.34 MHz), ^{19}F (16.1 and 21.34 MHz) and simulated [10] ^{31}P (at 21.34 MHz) NMR T_1 versus 1000/T in TMA-HFP in the entire temperature range studied.

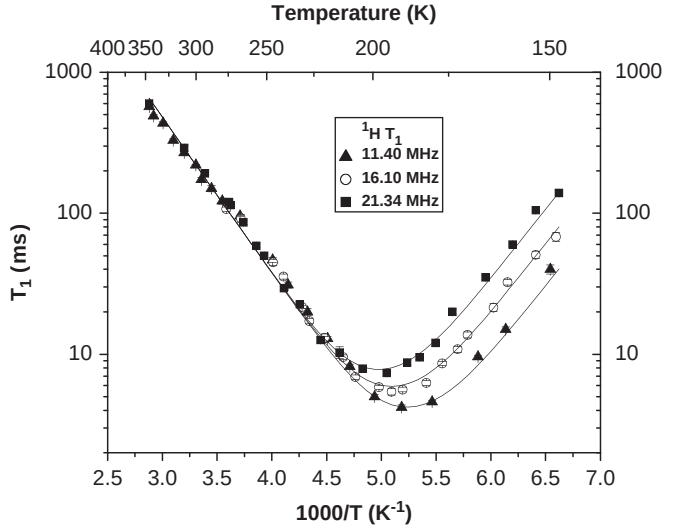

Fig. 3. ^{1}H NMR T_1 data for TMA-HFP at 11.40 MHz (▲), 16.10 MHz (○) and 21.34 MHz (■). Solid line represents the fit to Albert et al. [24] model.

from 350 K giving rise to a single asymmetric minimum at 190 K, unlike two minima exhibited by most of the tetramethylammonium compounds corresponding to TMA and CH_3 groups. Moreover, T_1 minimum of about 4.20, 5.42 and 7.35 ms observed, respectively at 11.4, 16.1 and 21.34 MHz, around 190 K, suggest that this minimum is due to simultaneous reorientations of both CH_3 and TMA groups with same correlation times. On further decrease in temperature, T_1 increases with a decrease in signal intensity (at all frequencies) enabling the measurements down to only 150 K. On further cooling, signal to noise ratio decreases drastically and signal vanishes completely below 150 K. On further cooling, the signal could not be observed even down to liquid helium temperature.

4.3. Theory

Tetramethylammonium ion has tetrahedral symmetry (similar to the NH_4^+ ion). It has three two-fold and four three-fold

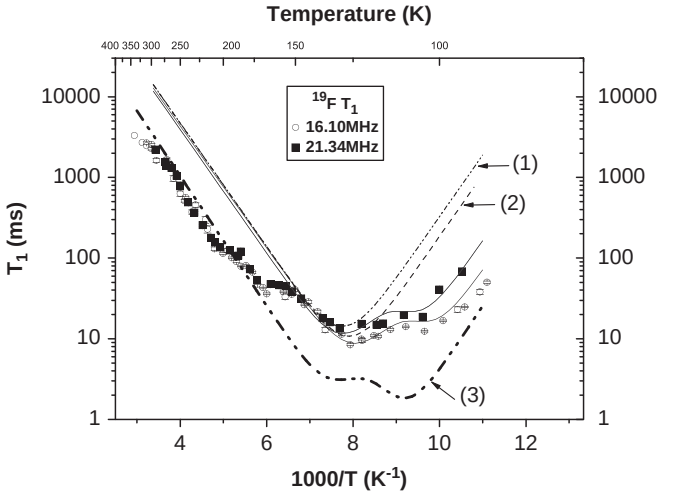

Fig. 4. ^{19}F NMR T_1 data for TMA-HFP at 16.10 MHz (○) and 21.34 MHz (■). Dotted lines show the ^{19}F T_1 simulations: Plot (1) at 21.34 MHz without considering the ^{1}H contribution, Plot (2) at 16.1 MHz without considering the ^{1}H contribution and Plot (3) at 16.1 MHz with 100% ^{1}H contribution to the PF_6 reorientation due to cross relaxation from proton. Solid lines represent the fit to Albert et al. model [6] with partial cross relaxation.

symmetry axes. T_1 behaviour in tetramethylammonium compounds can be explained using a modified Bloembergen, Purcell and Pound (BPP) approach [30], modified by Albert et al. [24]. In tetramethylammonium compounds, the two motions that mainly contribute to the relaxation are (a) reorientation of the CH_3 groups about their C_3 axes with correlation time τ_c and (b) isotropic tumbling of the TMA ion (whole cation) with a correlation time τ_{c1}. These motions modulate the intra-methyl and inter-methyl dipole–dipole interactions and facilitate the spin-lattice relaxation.

The intra-methyl proton–proton interaction is modulated by the reorientations of the methyl groups about their C_3 axes. The relaxation rate due to intra-methyl contribution is given by [24,31]

$$T_{1(\mathrm{intra})}^{-1} = \frac{9}{20}\frac{\gamma^4\hbar^2}{r^6}\left(f(\omega,\tau_{c2}) + \frac{1}{3}f(\omega,\tau_{c1})\right), \tag{2}$$

where

$$f(\omega,\tau_c) = \frac{\tau_c}{1+\omega_I^2\tau_c^2} + \frac{4\tau_c}{1+4\omega_I^2\tau_c^2} \tag{3}$$

and

$$\tau_{c2}^{-1} = \tau_c^{-1} + \tau_{c1}^{-1}. \tag{4}$$

In the above equations, $\gamma = 2.675\times10^4\,\mathrm{G^{-1}\,s^{-1}}$ is the nuclear gyromagnetic ratio of protons, 'τ' represents a correlation time of the motion and is assumed to obey the Arrhenius equation given by

$$\tau = \tau_0 \exp(E_a/RT). \tag{5}$$

Here τ_0 and E_a are the pre-exponential factor and activation energy of the corresponding motion, respectively.

The methyl group is considered as a three-spin system with each proton situated at the corners of the triangle and 'r' is the inter proton distance. Considering 'R' as the distance between the centres of the proton triangles, the relaxation rate due to the inter methyl proton-proton interaction modulated by the tumbling of the TMA ion, is given by [24,32]

$$T_{1(\mathrm{inter})}^{-1} = \frac{27}{20}\frac{\gamma^4\hbar^2}{R^6}f(\omega,\tau_{c1}). \tag{6}$$

Table 1
Motional parameters for TMA-HFP obtained from ^{1}H T_1 and ^{19}F T_1 fit to Eqs. (7) and (15), respectively

Symmetric group	Activation energy (kJ/mol)	Pre-exponential factor (10^{-13} s)
Methyl	16.8 (0.5)	2.81 (1)
TMA	22 (1)	0.15 (0.02)
PF_6	15 (1)	0.06 (0.01)

The effective relaxation rate is the sum of the relaxation rates due to intra-methyl and inter-methyl contributions and is given by

$$T_1^{-1} = T_{1(\text{intra})}^{-1} + T_{1(\text{inter})}^{-1} \tag{7}$$

which is

$$T_1^{-1} = Af(\omega, \tau_{c2}) + Bf(\omega, \tau_{c1}), \tag{8}$$

where

$$A = \frac{9}{20}\frac{\gamma^4\hbar^2}{r^6} \tag{9}$$

and

$$B = \frac{3}{20}\frac{\gamma^4\hbar^2}{r^6} + \frac{27}{10}\frac{\gamma^4\hbar^2}{R^6}. \tag{10}$$

Assuming that the TMA ion is an undistorted tetrahedron with C–H distance of 1.09 Å, C–N distance of 1.5 Å, the values of '*r*' and '*R*' are calculated to be 1.78 Å and 3.04 Å, respectively. Thus the values of A and B are found to be $A = 8.05 \times 10^9\,\text{s}^{-2}$ and $B = 4.61 \times 10^9\,\text{s}^{-2}$.

From Eq. (8) one expects a minimum of 20.27 ms corresponding to the TMA tumbling motion, for $\omega\tau_{c1} = 0.616$ and another minimum of 11.74 ms corresponding to the CH_3 group reorientation for $\omega\tau_c = 0.616$ at a Larmor frequency of 21.34 MHz. However, the present investigation reveals only one broad asymmetric minimum. Albert et al. model as given in Eq. (8) fits well to the present ^{1}H NMR T_1 data at all frequencies studied and the fit curves are shown in Fig. 3. The fit parameters (activation energies and pre-exponential factors) obtained for all frequencies are within the error limits (shown in the parentheses) and are given in Table 1.

Activation energies obtained from T_1 data analysis (16 and 22 kJ/mol for CH_3 and TMA groups, respectively) are consistent with that (<24 kJ/mol) obtained from second moment studies. However, these values are less than that for $((CH_3)_4N)_2SO_4$ (28 and 45 kJ/mol), $TMAClO_4$ (21.2 and 32.9 kJ/mol) [33] and $(CH_3)_4NX$ (X = Cl, Br and I) (23–28 and 37–54 kJ/mol) [24]. This indicates an increased freedom for the reorientation of the groups as compared to pure salts. CH_3 group activation energy observed in the present compound compare well with the reported value of 15–17 kJ/mol and the $N(CH_3)_4$ group activation energy is slightly lesser than the reported value of 30–37 kJ/mol, for $[(CH_3)_4N]_2MBr_6$ (M = Te, Sn and Pt) [26] and similar compounds [34–36].

(b) ^{19}F *NMR* T_1 *analysis*: Fig. 4 shows the ^{19}F NMR spin lattice relaxation time data at two Larmor frequencies (16.1 and 21.34 MHz). Initially ^{19}F T_1 decreases with decrease in temperature from 350 K giving rise to a single broad asymmetric minimum (around 115 K) at much lower temperatures compared to the proton minimum (around 190 K). On further decrease in temperature, T_1 increases with a decrease in signal intensity, at both the frequencies studied. Hence we could make measurements down to only 85 K below which the signal vanishes completely due to poor signal to noise ratio. No measurements were possible down to liquid helium temperatures.

4.4. Theory

The analysis of the fluorine relaxation time T_1 is rather complex compared to that of proton T_1. Gutowsky et al. [2] have investigated several MPF_6 compounds by ^{19}F NMR second moment and relaxation time studies. Albert and Gutowsky [6] have observed the cross relaxation effects between proton and fluorine using ^{1}H and ^{19}F NMR relaxation time studies in NH_4PF_6. ^{19}F spin lattice relaxation may occur due to the following contributions: (a) intra-ionic F–F interaction (b) intra-ionic F–H interaction (c) P–F interactions and (d) inter-ionic F–F interactions. Further as the Larmor frequencies of P and F differ by a factor of ≈0.432, P–F (inter molecular) cross relaxation may not play a significant role in relaxation process. The P–F contribution is only about 3% of the total and is neglected [10]. Cross relaxation between F and H is a prominent source for relaxation at least at higher temperatures, because the Larmor frequencies of F and H differ by a factor of only 1.063. Thus ^{19}F spin lattice relaxation occurs due to the magnetic dipole–dipole interactions modulated by (i) the random reorientations of the PF_6 ions and (ii) isotropic reorientations of the TMA ion and methyl group.

^{19}F T_1 data in the temperature range (350–155 K) follows that of ^{1}H T_1. However, below 155 K, cross relaxation effect between proton and fluorine reduces and ^{19}F T_1 follows the same trend as that of phosphorous T_1. The simulated (using the motional parameters of the PF_6 reorientation as reported by Reynhardt et al. [10]) ^{31}P NMR T_1 data at 21.34 MHz are included in Fig. 2. for the sake of comparison and same motional parameters are used for the analysis of ^{19}F T_1 data.

In the high temperature region ($T > 155$ K), the PF_6 ion reorientation rate gets modulated by ^{19}F and ^{1}H cross relaxation effects. Correspondingly, ^{19}F T_1 shows reduced T_1 and a shallow minimum around the same temperature where the proton T_1 minimum is observed. The relaxation rate for the fluorine nucleus due to proton group motion can then be written as [23,37,38]

$$\frac{1}{T_1^F} = R_F = \frac{2}{3}\gamma_F^2\Delta M_{FF}g(\omega_F, \tau_F) + \frac{1}{2}\gamma_F^2\Delta M_{FP}g_F(\omega_{PF}, \tau_F) + \frac{5}{48}\gamma_F^2\Delta M_{FH}g_F(\omega_{HF}, \tau_F) + \frac{3}{16}\gamma_F^2\Delta M'_{FH}g_F(\omega_{HF}, \tau_F), \tag{11}$$

where

$$g(\omega_F, \tau_F) = \frac{\tau_F}{1+\omega_F^2\tau_F^2} + \frac{4\tau_F}{1+4\omega_F^2\tau_F^2} \tag{12}$$

$$g_F(\omega_{PF}, \tau_F) = \frac{\tau_F}{1+(\omega_P-\omega_F)^2\tau_F^2} + \frac{3\tau_F}{1+\omega_F^2\tau_F^2} + \frac{6\tau_F}{1+(\omega_P+\omega_F)^2\tau_F^2} \tag{13}$$

and

$$g_F(\omega_{HF}, \tau_F) = \frac{\tau_F}{1+(\omega_H-\omega_F)^2\tau_F^2} + \frac{3\tau_F}{1+\omega_F^2\tau_F^2} + \frac{6\tau_F}{1+(\omega_H+\omega_F)^2\tau_F^2}. \tag{14}$$

In the above equations, $\gamma_F = 2.5166 \times 10^4\,\text{G}^{-1}\,\text{s}^{-1}$ is the gyromagnetic ratio of the fluorine nucleus; τ_F is the correlation time describing the orientations of the PF_6 ions; ω_F, ω_H and ω_P are Larmor frequencies. For $\omega_F = 21.34$ MHz, the corresponding ω_H is 22.68 MHz and ω_P is 9.18 MHz. The quantities ΔM_{FF} and ΔM_{FP} in Eq. (11) are the changes in the apparent second moment of the fluorine resonance associated with the random reorientations of the PF_6 ions. The intra-ionic contributions to ΔM_{FF} and ΔM_{FP} depend upon the P–F bond distance in the octahedral ion. If one takes this value as 1.58 Å [12], these two contributions are found

be 12 and 1.7 G^2, respectively [2]. ΔM_{FH} and $\Delta M'_{FH}$ represent the reduction in second moment for the H–F interactions for spherically averaged TMA ion and stationary PF_6 ions, respectively. The ΔM_{FH} and $\Delta M'_{FH}$ values are assumed to be 3.1 and 3.8 G^2, respectively, for tetrahedral symmetry for the cation [6]. Considering these factors, one can rewrite Eq. (11) as

$$\frac{1}{T_1^F} = 5.066 \times 10^9 g(\omega_F, \tau_F) + 0.5383 \times 10^9\, g_F(\omega_{PF}, \tau_F) + c_1 2.045 \times 10^9\, g_F(\omega_{HF}, \tau_F) + c_2 4.5126 \times 10^9\, g_F(\omega_{HF}, \tau_F). \quad (15)$$

A least square fit to Eq. (15) to the experimental T_1 data is shown in Fig. 4. In particular, the minimum at $(\omega_H - \omega_F)\ \tau_F \approx 1$ (i.e., $\tau_F \approx 1.17 \times 10^{-7}$ s, which occurs at 108 K) and a hump at $\omega_F \tau_F \approx 1$ (i.e., $\tau_F \approx 7.46 \times 10^{-8}$ s, which occurs at 111 K) which are expected [39] from the form of Eq. (14) are well reproduced in the experimental fluorine relaxation time curve. If the contribution from the proton is neglected, i.e., considering only first two terms in Eq. (11), one gets single T_1 minimum of 13.34 ms at 21.34 MHz and 10.06 ms at 16.1 MHz as shown by the dotted lines (Plot (1) and Plot (2)) in Fig. 4. Further, if one considers proton relaxation is efficient throughout the temperature range studied, then the ^{19}F NMR T_1 data should have followed the thick dotted line (Plot (3)) shown in Fig. 4. However, experimental T_1 data follow this trend from room temperature down to about 155 K, below which it deviates significantly. It is interesting to note that, at the same temperature (155 K), the ^1H NMR signal becomes very weak and then vanishes completely as observed both in second moment as well as T_1 measurements. Considering all these factors, one can conclude that both methyl and TMA groups start freezing below this temperature. However, there appears to be a finite contribution from some protons, which are actively relaxing fluorine nuclei. The best-fit parameters to Eq. (15) are given in Table 1. Considering this model, a least square fit to the present experimental results, yield values of C_1 (0.089) and C_2 (0.1) indicating that only a fraction of the total number of protons contributes to the ^{19}F relaxation. Even though 90% of the protons belonging to TMA and CH_3 group are frozen, about 10% of the protons are still active. It is reported in the literature [7] that a small fraction of the PF_6 ions do form hydrogen bonds with the cation. This proposition is also supported by the fact that rigid lattice second moment is not obtained at 155 K implying that some protons (about 10%) appear to be hydrogen bonded to PF_6 ions having a distributed correlation times and hence able to relax the fluorine nuclei down to much lower temperatures. Also, Eqs. (11)–(15) suggest that the linear portions of the high temperature side of the ^1H T_1 and ^{19}F T_1 minima should yield almost same activation energy. Indeed, the high temperature linear portion of the ^{19}F T_1 data gives activation energy of 22.6 (0.5) kJ/mol, in excellent agreement with that obtained from the high-temperature ^1H T_1 data which is 22 ($\pm$1) kJ/mol. Similar behaviour is observed by McDowell et al. [38] in $(CH_3)_3NPF_5$.

Present ^{19}F T_1 results yield motional parameters of the PF_6 reorientations, which are in excellent agreement with those reported by Reynhardt et al. [10] from ^{31}P T_1 analysis. However, contrary to the ^{31}P T_1 analysis, the present T_1 data do not seem to be affected by the existence of two phases, one with imperfections and another without imperfections. This may be due to the strong spin diffusion active among the fluorine groups that would mask the presence of imperfections and also the immediate neighbourhood of the cation might not have changed to that extent.

It is interesting to compare NMR results of other alkali hexafluorophosphates with the present studies. It is evident that, in APF_6 compounds, changing the cation (A) results in a change of activation energy of the PF_6 ion. Activation energy for PF_6 motion in TMA-HFP is found to be less than that of all other alkali and ammonium hexafluorophosphates [2,6], resulting in a ^{19}F T_1 minimum around 115 K. Table 2 gives a comparison of E_a along with the corresponding ionic radii. A general trend of decrease in E_a for PF_6 motion is observed with increase in the ionic radii [40] of the cation A, except for K ion. This could be correlated to the increased freedom for PF_6 motion. On the other hand, Svare and Ain el Hiah Abd el Haleem [36] have reported that in $(NH_4)_2BF_6$ (B = Ti, Ge and Si), with A cation remaining the same (NH_4 ion in this case), an increase in the 'B' cation radius results in a decrease of activation energy of the NH_4 ion due to increase of the cell volume. Hence we speculate that, different tetramethylammonium hexafluorometallates are promising candidates to undertake similar studies. Since ^1H M_2 in the present compound has not reached the rigid lattice value even at 155 K, it is interesting to compare the temperatures of the motional narrowing in similar compounds. The ^1H M_2 measurements have shown that in NH_4BF_4 [39] and NH_4PF_6 [6], the motional narrowing occurs at temperatures less than 55 and 77 K, respectively and M_2 have not reached the corresponding rigid lattice value even at very low temperatures. This implies that the motion of the molecular groups is not frozen completely down to these temperatures.

Table 2
Comparison of activation energies for the PF_6 ion with cation ionic radius in APF_6 compounds

Cation A	Ionic radius (Å)	PF_6 ion activation energy (kJ/mol)
Sodium	1.02	33
Potassium	1.37	46
Ammonium	1.47	17
Rubidium	1.52	17
Tetramethylammonium	3.01	15

5. Conclusions

^1H T_1 measurements at all frequencies have shown single asymmetric minimum, which is attributed to simultaneous onset of reorientation motion of both CH_3 and $(CH_3)_4N$ groups, which is also supported by the observation of a single plateau in second moment measurements. Cross relaxation between proton and fluorine has been invoked to explain the observed ^{19}F T_1 data. Single exponential recovery of magnetisation, in spite of cross relaxation, might be due to the strong spin diffusion among different reorienting groups. At low temperatures, only a small fraction of hydrogen bonded protons to PF_6 ions appear to relax fluorine nuclei. The observed lower activation energy for the PF_6 motion is attributed to the increase of the cation radius in hexafluorophosphates.

Acknowledgments

Our research is supported by grants from Department of Atomic Energy (DAE-BRNS) and University Grants Commission, Government of India.

References

[1] G.R. Miller, H.S. Gutowsky, J. Chem. Phys. 39 (8) (1963) 1983–1994.
[2] H.S. Gutowsky, S. Albert, J. Chem. Phys. 58 (12) (1973) 2452–5446.
[3] H. Ono, S. Ishimaru, R. Ikeda, H. Ishida, Bull. Chem. Soc. Jpn. 72 (1999) 2049–2054.
[4] H. Ono, S. Ishimaru, R. Ikeda, H. Ishida, Ber. Bunsenges. Phys. Chem. 102 (1998) 650–655.

[5] M. Grotte, A. Kozak, A.E. Kozil, Z. Pajak, J. Phys. Condens. Matter 1 (1989) 7069–7085.
[6] S. Albert, H.S. Gutowsky, J. Chem. Phys. 59 (7) (1973) 3585–3594.
[7] A.M. Heyns, W.H.J. De Beer, Spectrochim. Acta 39A (7) (1983) 601–607.
[8] L.A.K. Staveley, N.R. Grey, M.J. Layzell, Z. Naturforsch. A 18 (1963) 148.
[9] W.H.J. De Beer, A.M. Heyns, Spectrochim. Acta 37A (1981) 1099–1107.
[10] E.C. Reynhardt, S. Jurga, K. Jurga, Chem. Phys. Lett. 194 (1992) 410–414.
[11] L. Ugalde, J.C. Bernede, M.A. Del Valle, R.F. Díaz, P. LeRay, United States Patents 6773822, 20040110868: OSTI ID: 4572627, AD0757883, J. Appl. Polym. Sci. 84 (10) (2002) 1799–1809;
A.-N. Chowdhury, Y. Kunugi, Y. Harima, K. Yamashita, Thin Solid Films 271 (1995) 1–3.
[12] Y. Wang, L.D. Calver, S.K. Brownstein, Acta Crystallogr. B 36 (1980) 1523.
[13] K.J. Mallikarjunaiah, R. Damle, Vignana Bharathi 11 (1) (2005) 50–55.
[14] B.V.S. Murthy, NMR study of molecular dynamics and phase transitions in selenates and plumbates of R_2MX_6 family, Ph.D. Thesis, Department of Physics, Indian Institute of Science, Bangalore, India, 1993.
[15] J.H. Van Vleck, Phys. Rev. 74 (1948) 1168–1183.
[16] R. Goc, J. Magn. Reson. 132 (1998) 78–80.
[17] R. Goc, Comp. Phys. Comm. 162 (2004) 102–112.
[18] R. Goc, Z. Naturforsch. 58a (2003) 537–540.
[19] D.J. Blears, S.S. Danyluk, E. Bock, J. Phys. Chem. 72 (6) (1968) 2269–2270.
[20] A. Migdał-Mikuli, E. Mikuli, Ł. Hetmańczyk, I. Natkaniec, K. Hołderna-Netkaniec, W. Łasocha, J. Solid State Chem. 174 (2003) 357–364.
[21] T. Tsang, D.B. Utton, J. Chem. Phys. 64 (9) (1976) 3780–3783.
[22] E.R. Andrew, P.C. Canepa, J. Magn. Reson. 7 (1972) 429–441.
[23] A. Abragam, The Principles of Nuclear Magnetism, Oxford University Press, New York, 1961.
[24] S. Albert, H.S. Gutowsky, J.A. Ripmeester, J. Chem. Phys. 56 (7) (1972) 3672–3676.
[25] M. Mahajan, B.D. Nageswara Rao, J. Phys. C Solid State Phys. 7 (1974) 995–1000.
[26] L.S. Prabhumirashi, R. Ikeda, D. Nakamura, Ber. Bunsenges. Phys. Chem. 85 (1981) 1142–1148.
[27] S. Sato, R. Ikeda, D. Nakamura, Ber. Bunsenges. Phys. Chem. 86 (1982) 936–941.
[28] K.J. Mallikarjunaiah, K.C. Paramita, K.P. Ramesh, R. Damle, Solid State Nucl. Magn. Reson. 32 (1) (2007) 11–15.
[29] K.J. Mallikarjunaiah, K. Jugeshwar Singh, K.P. Ramesh, R. Damle, Magn. Reson. Chem. 46 (2) (2007) 110–114.
[30] N. Bloembergen, R.V. Purcell, R.V. Pound, Phys. Rev. 73 (7) (1948) 679–712.
[31] T. Akai, N. Nakamura, H. Chihara, J. Chem. Soc. Faraday Trans. 89 (9) (1993) 1339–1343.
[32] D.E. Oreilly, T. Tsang, J. Chem. Phys. 46 (1967) 1291–1300.
[33] T. Tsuneyoshi, N. Nakamura, H. Chihara, J. Magn. Reson. 27 (1977) 191–195.
[34] Y. Furukawa, H. Kiriyama, R. Ikeda, Bull. Chem. Soc. Jpn. 54 (1981) 103–108.
[35] S. Senthil Kumaran, K.P. Ramesh, J. Ramakrishna, Mol. Phys. 99 (16) (2001) 1373–1380.
[36] Ivar Svare, Ain el Hiah Abd el Haleem, Phys. Scr. 19 (1979) 351–354.
[37] D.E. Oreilly, E.M. Peterson, T. Tsang, Phys. Rev. 160 (1967) 333–342.
[38] C.A. McDowell, P. Raghunathan, D.S. Williams, J. Magn. Reson. 32 (1978) 57–69.
[39] A.P. Caron, D.J. Huttner, J.L. Ragle, L. Sherk, T.R. Stengle, J. Chem. Phys. 47 (8) (1967) 2577–2583.
[40] D. R. Lide, Handbook of Chemistry and Physics, 84th ed, CRC Press, Boca Raton, FL, 2003.